Article

Non-Flammable Epoxy Composition Based on Epoxy Resin DER-331 and 4-(β-Carboxyethenyl)phenoxy-phenoxycyclotriphosphazenes with Increased Adhesion to Metals

Anastasia Konstantinova [1], Pavel Yudaev [1], Aleksey Shapagin [2], Darya Panfilova [1], Aleksandr Palamarchuk [1] and Evgeniy Chistyakov [1,*]

[1] Department of Chemical Technology of Plastics, Mendeleev University of Chemical Technology of Russia, Miusskaya Sq. 9, 125047 Moscow, Russia

[2] A.N. Frumkin Institute of Physical Chemistry and Electrochemistry, Russian Academy of Sciences, 119071 Moscow, Russia

* Correspondence: ewgenijj@rambler.ru

Abstract: Functional cyclophosphazenes have proven to be effective modifiers of polymer materials, significantly improving their performance properties, such as adhesive characteristics, mechanical strength, thermal stability, fire resistance, etc. In this study, 4-(β-carboxyethenyl)phenoxy-phenoxycyclotriphosphazenes (CPPP) were obtained by the condensation of 4-formylphenoxy-phenoxycyclotriphosphazene with malonic acid. Its structure was studied using ^{31}P, ^1H, and ^{13}C NMR spectroscopy and MALDI-TOF mass spectrometry, and the thermal properties were determined by DSC and TGA methods. Molecular modeling using the MM2 method showed that CPPPs are nanosized with diameters of spheres described around the molecules in the range of 1.34–1.93 nm, which allows them to be classified as nanosized structures. The epoxy resin DER-331 was cured with CPPP, and the conversion of epoxy groups was assessed using IR spectroscopy. Using optical interferometry, it was shown that CPPPs are well compatible with epoxy resin in the temperature range from 80 to 130 °C. It was established that the cured epoxy composition was fire resistant, as it successfully passed the UL-94 vertical combustion test due to the formation of porous coke during the combustion process and also had high heat resistance and thermal stability (decomposition onset temperature about 300 °C, glass transition temperature 230 °C). The composition has low water absorption, high resistance to fresh and salt water, fire resistance, and adhesive strength to steel and aluminum (11 ± 0.2 MPa), which makes it promising for use as an adhesive composition for gluing parts in the shipbuilding and automotive industries, the aviation industry, and radio electronics.

Keywords: phosphazene; glue; aluminum; steel; non-flammable; fire resistance; mutual solubility; heat resistance; adhesion strength; nanosized structure

1. Introduction

Today, polymers are the most widely used material in many areas of industry and the national economy. An important place among polymers is occupied by epoxy resins, which are used in innovative technologies [1], construction [2], and electronics [3], as well as for the creation of environmentally friendly materials [4], nanocomposites with improved performance characteristics [5], biodegradable composites [6], and composites with increased wear and impact resistance [7]. However, the disadvantage of epoxy polymer materials is their flammability due to the organic nature of most of them [8]. To solve the problem of the flammability of materials based on epoxy resins (composite materials, adhesives, etc.), flame retardants are used. They are divided into additive- and reactive-type flame retardants according to the nature of their interaction with polymers.

Among the flame retardants, the most promising are reactive-type flame retardants, since they are better compatible with the polymer matrix in contrast to additive-type flame retardants, such as aluminum butyl methylphosphinate [9], a mixture of ammonium polyphosphate and aluminum hydroxide [10], zinc hydroxystannate, and carbon nanotubes [11].

In terms of composition, halogen-containing flame retardants are among the most common, since they are cheap and effective [12]. For example, in [13], a fluorinated diamine based on the natural isoflavone daidzein was used as an epoxy resin hardener.

However, the disadvantage of halogen-containing flame retardants is the formation of toxic volatile substances and a large amount of smoke during the combustion process. Therefore, special methods are being developed to remove halogens from waste polymer materials so as not to harm the environment [14].

Another approach is to replace halogen-containing flame retardants with silicon-, phosphorus-, and/or nitrogen-containing ones, as well as their hybrids. Among silicon-containing flame retardants, silicone resins are used [15], and among phosphorus- and/or nitrogen-containing ones, a mixture of diammonium hydrogen phosphate and urea [16], derivatives of DOPO [17–19] and DOPS [20], the product of the reaction of phenyldichlorophosphate with N-hydroxyethyl acrylamide [21], a reaction product of melamine and 2-[(5-oxo-6H-phosphanthridin-5-yl)methyl]butanedioic acid [22], etc. However, phosphorus-containing flame retardants, in particular organophosphates, have neurotoxic and carcinogenic properties, which requires their monitoring in the environment [23].

Phosphazenes are a class of organic–inorganic compounds with chemical lability, which provides them with a wide range of valuable properties and applications. Phosphazenes are non-toxic and can even be used in pharmaceuticals [24–26]. Porous polymers based on phosphazenes are used in environmentally friendly sorption processes [27] and industrial catalysis [28], and some cyclophosphazenes even have an anti-corrosion effect towards metals, which is important in the manufacture of metal-containing composites [29].

Accordingly, phosphazenes and metal complexes based on them are promising flame retardants for various polymers, such as polylactic acid [30], mixtures of cotton and polyamide [31], and, of course, epoxy resins [32,33]; this is due to the cooperative effect of phosphorus atoms and the nitrogen in phosphazenes. During the combustion process, inert gases are formed in the gas phase, which reduces the oxygen concentration. Free phosphorus radicals are also generated, which leads to the quenching of hydrocarbon-free radicals and the cessation of combustion [34]. In particular, the addition of only 1 wt. % cyclotriphosphazene-based Schiff base increases the oxygen-limiting index of 4,4′-diaminodiphenylmethane-cured epoxy resin by 17% [35].

It seems promising to use carboxyl-containing cyclophosphazenes as a hardener for epoxy resins, which will simultaneously act as a reactive fire retardant. However, a disadvantage of carboxyl-containing cyclophosphazenes is their poor compatibility with epoxy resins due to the formation of hydrogen bonds involving carboxyl groups, which was shown in the example of hexakis-4-(β-carboxyethenylphenoxy)cyclotriphosphazene [36]. Therefore, for the purpose of this work, to improve the compatibility of carboxyl-containing cyclophosphazenes with epoxy resins, it was decided to reduce the content of carboxyl groups in the above cyclophosphazene by replacing part of the β-carboxyethenylphenoxy groups with phenoxy radicals. It was assumed that the synthesized modifier 4-(β-carboxyethenyl)phenoxy-phenoxycyclotriphosphazene (CPPP) would be well compatible with the industrial epoxy-diane resin DER-331 and would be its hardener. In addition to reduced flammability, the epoxy compositions obtained in this way could have high adhesive strength to metals due to the ability of carboxyphosphazenes to form metal complexes, which would make it possible to use the development for the production of non-flammable metal adhesives, metal-containing composites, and special-purpose putties.

2. Materials and Methods

2.1. Materials

The epoxy resin DER-331 was purchased from DOW Chemical Company (Berlin, Germany). Malonic acid (MA), anhydrous (99%), pyridine, anhydrous (99.8%), piperidine (99%), phenol (99%), 4-hydroxybenzaldehyde (98%), tetrahydrofuran (THF), anhydrous (≥99.5%), potassium carbonate, anhydrous (≥99%), chloroform, anhydrous (≥99.5%), the deuterated solvent (DMSO-d_6 and CDCl$_3$) for NMR analysis, potassium hydroxide, and hydrochloric acid (37%) were purchased from Sigma-Aldrich (Saint Louis, MO, USA). Hexachlorocyclotriphosphazene (HCP, 99%) was purchased from Fushimi Pharmaceutical Co., Ltd. (Marugame, Kagawa Prefecture, Japan).

2.2. Methods

^{1}H, ^{31}P, and ^{13}C NMR spectra were recorded with an Agilent/Varian Inova 400 spectrometer (Agilent Technologies, Santa Clara, CA, USA) at 400.02 MHz, 161.94 MHz, and 100.60 MHz, respectively, and root temperature. DMSO-d_6 or CDCl$_3$ were used as solvents.

The mass spectrum was recorded with a Microflex LRF mass spectrometer (Bruker Daltonic GmbH, Leipzig, Germany).

IR spectra were recorded using a Nicolet 380 spectrometer (Thermo Fisher Scientific, Waltham, MA, USA) in the spectral range 4000–500 cm^{-1} with a wavenumber accuracy of 0.01 cm^{-1}.

Differential-scanning calorimetry (DSC) and thermogravimetric analysis (TGA) measurements were performed using the NETZSCH STA 449F1 (Erich NETZSCH GmbH & Co. Holding KG, Selb, Germany) instrument (10 °C min^{-1}). Argon was used as a purge gas.

The images of the coke cap were obtained with a scanning electron microscope TES-CAN VEGA 3 XMU in secondary electron mode. To obtain images, a fragment of a coke cap sample was attached to a holder with conductive tape, and the edges of the sample were coated with silver-based glue. Then, a 20 nm thick layer of gold was deposited under vacuum.

The shear strength of the adhesive bond was determined according to ISO 4587-79 [37] on a 50ST Tinius Olsen universal testing machine (Tinius Olsen TMC, Horsham, PA, USA) with a traverse speed of 10 mm/min. Steel plates were used as the bonded material (steel grade St3, analog: A57036 (USA), SS330 (Japan), DC03 (Germany)).

The test sample consisted of two strips of sheet metal glued together with an overlap. The sample prepared for testing was installed along the marks in the clamps of the testing machine so that the longitudinal axis of the sample coincided with the axis of application of the load. The tests were carried out by gradually increasing the load until the sample was destroyed. The highest load achieved during the test was recorded. The strength of adhesive joints in shear is expressed by the magnitude of the breaking stress in shear, calculated by the formula

$$\tau = \frac{P}{F}$$

where P is the breaking load, N, and F is the gluing area, m^2, calculated by the formula

$$F = l \times b$$

where l is the length of the overlap, m, and b is the width of the overlap, m.

Resistance to combustion for the prepared compositions was determined according to the UL-94 test. The test sample was attached to the upper end with a grip of 6 mm of its length with its longitudinal axis in a vertical position. The lower end of the sample was 300 ± 10 mm above the horizontal uncompressed layer of cotton with approximate dimensions of 50 × 50 × 6 mm and a mass of no more than 0.08 g. The burner, with the central axis of the pipe in a vertical position, was installed at a distance from the sample. The burner was kept for at least 5 min to stabilize the condition. After applying the flame to the sample for (10 ± 0.5) s, the burner was immediately removed to prevent its influence

on the sample and, at the same time, a stopwatch was turned on to measure the residual combustion time t_1 in seconds. After the residual combustion of the test sample stopped, the test flame was immediately brought under the sample for a time (10 ± 0.5) s, holding the central axis of the burner pipe in a vertical position. The top of the burner should be at a distance of (10 ± 1) mm from the bottom edge of the remaining part of the sample. After the second application of the flame to the test sample for $(10 + 0.5)$ s, the burner was immediately extinguished or removed to such a distance as to prevent its influence on the sample, and at the same time, using a stopwatch, the residual burning time was measured to the nearest second t_2 and residual smoldering time t_3 of the sample.

The water absorption and water solubility content of the test compositions were determined according to ISO 62:2008 [38].

The salt resistance of the compositions was determined according to ISO 175:2010 [39].

The optical interferometry technique was used to evaluate the compatibility of CPPP with epoxy resin. The measurements were carried out using an ODA-2 laser diffusion meter. The method is based on the phenomenon of multi-beam interference from two surfaces of polished glass plates forming an angle of $\approx 2°$. The inner surfaces of the lenses were coated with a layer of translucent metal with a high reflectivity. Phosphazene powder was placed between the glass plates and thermostated above its glass transition temperature, and the resin was injected into the wedge at the experimental temperature. The moment of contact of the fronts was considered the beginning of the process of diffusion mixing. Interdiffusion measurements were carried out in isothermal mode. To assess the compatibility of the components, the temperature was increased and decreased in steps of 10 °C in the range from 20 to 130 °C.

The chemical structures of cyclotriphosphazenes were modeled in ChemBioDraw Ultra v10.0, and the lowest energy conformations were calculated in ChemBio3D Ultra using the MM2 force field with a minimum root mean square gradient of 0.1.

Statistical analysis: The average values of the performance characteristics of various samples were compared using two-way ANOVA followed by Tukey's special analysis for multiple comparisons.

2.3. Synthesis of 4-Formylphenoxy-Phenoxycyclotriphosphazene (FPPP)

In a 50 mL three-neck flask, 2 g (0.0058 mol) of HCP and 1.6 g (0.0172 mol) of phenol are sequentially dissolved in 20 mL of THF, after which 2.4 g (0.0172 mol) of potassium carbonate is added to the mixture. The reaction is carried out by stirring for 6 h at the boiling point of the solvent. As a result, chlorophenoxycyclotriphosphazenes (CPP) are formed, which are not isolated. Then, 2.1 g (0.0172 mol) of 4-hydroxybenzaldehyde and 2.4 g (0.0172 mol) potassium carbonate are added to the reaction mixture and the process is continued with the solvent boiling for another 6 h. Upon completion, the suspension is filtered, and the product is precipitated with water. The precipitate is dissolved in chloroform and washed successively with a 0.1 M aqueous solution of potassium hydroxide and distilled water. Then, the solvent is distilled off, and the residue is dried in a vacuum oven to constant weight. Product yield: 4.5 g. ^{31}P NMR (CDCl$_3$, ppm): 8.8–9.5 (m). ^{1}H NMR (CDCl$_3$, ppm): 6.6–7.8 (m, CHAr) and 9.9 (s, CHO).

2.4. Synthesis of 4-(β-Carboxyethenyl)Phenoxy-Phenoxycyclotriphosphazene (CPPP)

In a 50 mL three-neck flask equipped with a stirrer and a reflux condenser, 1 g of the FPPP compound (0.0013 mol) and 0.8 g (0.0078 mol) of MA are sequentially dissolved in 10 mL of pyridine, with 2 drops of piperidine added. The synthesis is carried out at the boiling point of the solvent until the release of CO$_2$ bubbles ends. Then, while stirring, the solution is poured into a glass with 50 mL of 1 M hydrochloric acid; the precipitate is filtered and washed several times with distilled water, and then dried in a vacuum oven to constant weight. Yield: 1 g. ^{31}P NMR (DMSO-d_6, ppm): 9.8–10.3 (m). ^{1}H NMR (DMSO-d_6, ppm): 6.4–6.6 (d, =CH-COOH), 6.7–7.5 (m, CHAr), 7.7–7.8 (d, Ar-CH=), and 7.8–7.9 (m,

CHAr). MALDI-TOF (m/z): 834.12 (4-Phen/2-Carb + H$^+$), 904.10 (3-Phen/3-Carb + H$^+$), and 974.15 (4-Carb/2-Phen + H$^+$). FTIR (cm^{-1}, ATR): 1150–1240 (P = N).

2.5. Preparation of Composition and Test Samples Based on CPPP and DER-331

Seven grams of CPPP is ground in a porcelain mortar; five grams of DER-331 is added and ground thoroughly to a paste. The paste is placed in appropriate molds or on metal plates and evenly distributed on the required surface. The plates with the applied paste are connected and pressed tightly. The samples are placed in a heating cabinet and heated stepwise: 2 h at 80 °C, 2 h at 100 °C, and 13 h at 140 °C.

3. Results and Discussion

To obtain carboxyphosphazenes with a reduced content of carboxyl groups, the simplest and most accessible is ordinary phenol, which was taken in a three-fold molar excess relative to HCP. The synthesis of 4-(β-carboxyethenyl)phenoxy-phenoxycyclotriphosphazenes (CPPP) was carried out according to the scheme presented in Figure 1.
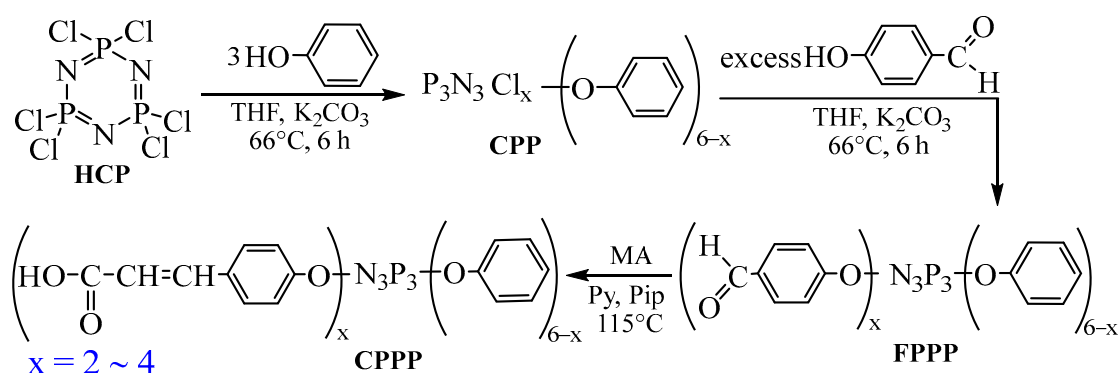

Figure 1. Diagram of obtaining CPPP.

The preparation of derivatives with exactly three carboxyl groups per phosphazene molecule is due to the fact that with a lower content of these groups during the curing of industrial epoxy resins, the formation of a network structure will be impossible. This is due to the fact that resins usually contain two epoxy groups per molecule, and carboxyl groups under curing conditions are not able to react with hydroxyl groups that are formed during the opening of oxirane rings. With a higher content of carboxyl groups, the solubility of phosphazene in the resin deteriorates, which prevents the formation of a homogeneous system and the production of material of proper quality.

The chlorine substitution reaction in phosphazene was carried out stepwise in order to regulate more clearly the composition of the resulting products, since with the simultaneous introduction of a mixture of phenolates, due to their different reactivity, the final products may be heterogeneous in composition.

The order of introduction of phenolates is determined by a practical approach. Since the sodium salt of phenol is soluble in THF but the phenolate of 4-hydroxybenzaldehyde is not, then the purification from the excess salt after the synthesis is carried out by conventional filtration. Therefore, the sodium salt of phenol is introduced first and completely consumed.

After treating HCP with the sodium salt of phenol, in the phosphorus NMR spectrum of the resulting CPP, in addition to the signals of the target tri-phenoxy-tri-chlorocyclotriphosphazene, there are also signals of di- and tetra-substituted aryloxyphosphazenes; according to the integrated intensities, their content in the mixture is 20 and 9 mol. %, respectively (Figure 2A).
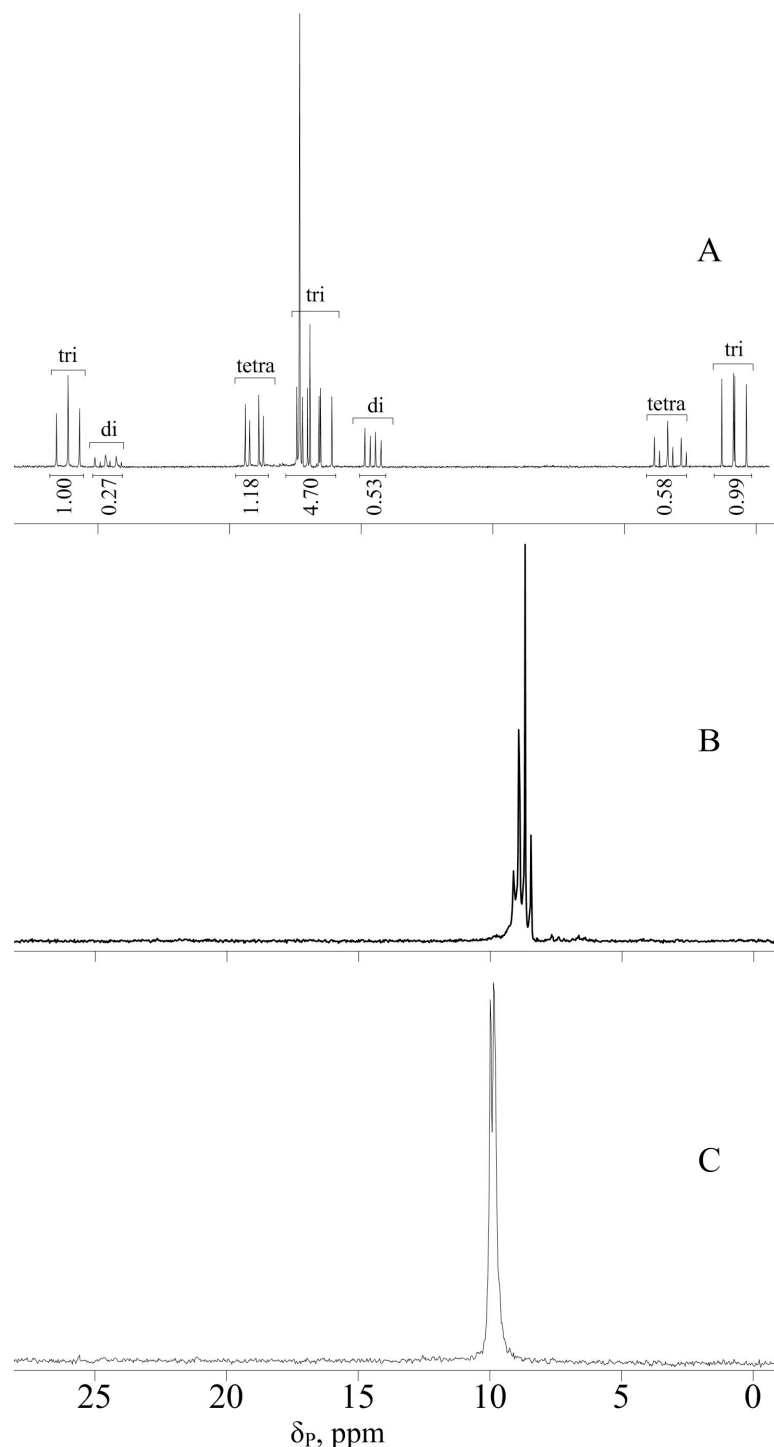
Figure 2. ^{31}P NMR spectra of products CPP (**A**), FPPP (**B**), and CPPP (**C**).

Upon subsequent addition of *p*-hydroxybenzaldehyde phenolate to CPP, the resulting FPPP was also analyzed by ^{31}P NMR spectroscopy (Figure 2B). The position of the signal on the scale was in the region of 8.8–9.5 ppm, confirming the completeness of chlorine substitution in hexachlorocyclotriphosphazene; however, instead of the expected singlet, the signal is a multiplet. This is explained by the fact that FPPP, like CPP, is a mixture of compounds with different contents of phenoxy and formylphenoxy groups on the phosphazene ring, with different effects on phosphorus atoms due to mesomeric effects. Based on the ratio of the integral intensities of the protons of formyl groups and aromatic rings shown in the ^{1}H NMR spectrum of FPPP (Figure 3A), we can conclude that, on

average, the content of phenoxy groups and p-formylphenoxy groups in the resulting product is the same.
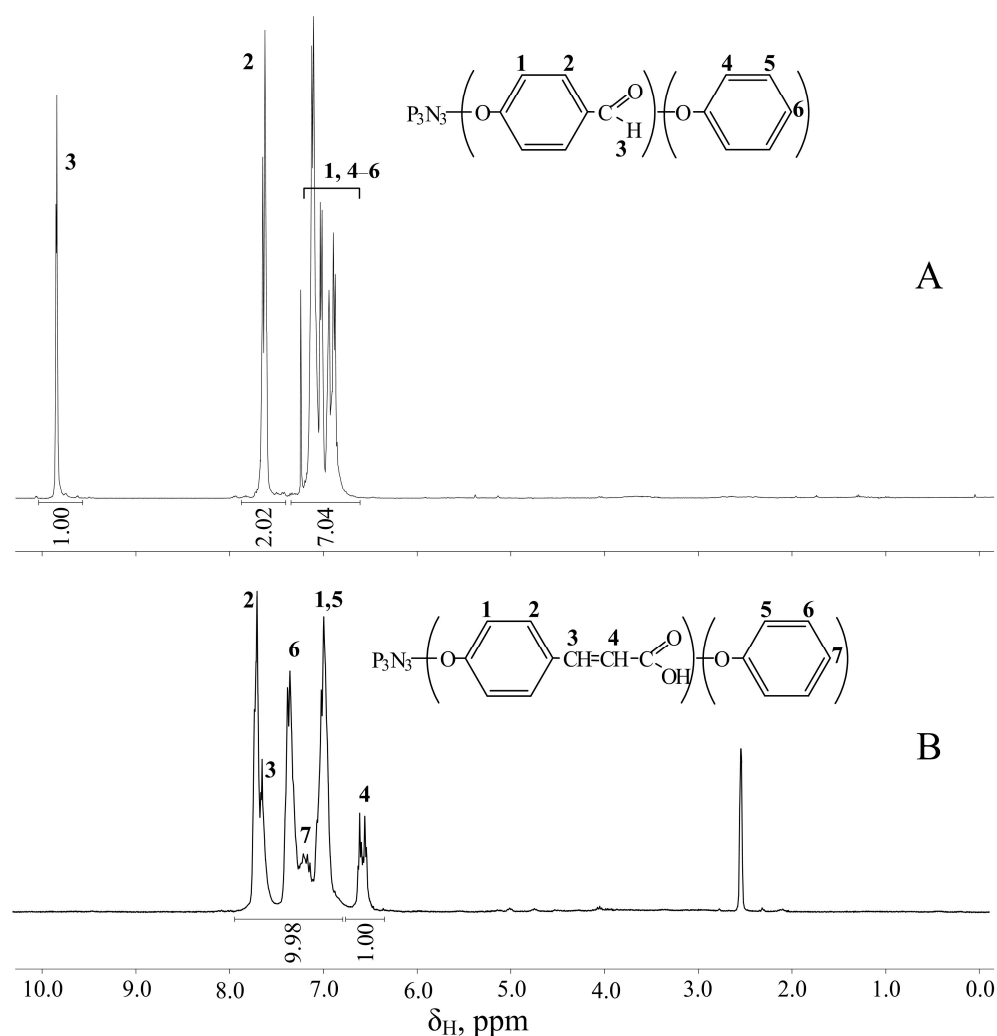

Figure 3. ^{1}H NMR spectra of FPPP (**A**) and CPPP (**B**).

At the next stage, FPPP was treated with malonic acid with the conversion of aldehyde groups into carboxyethenyl groups, which is indirectly evidenced by the disappearance of the signal of protons of carbonyl groups in the ^{1}H NMR spectrum of the resulting CPPP (Figure 3B). However, due to the deuterium exchange of acidic protons with d-DMSO, it is not possible to determine the presence of carboxyl groups in the resulting compounds from the proton spectrum. These groups were detected using ^{13}C NMR spectroscopy; in the CPPP spectrum in the region of 168.3 ppm, there is a peak associated with the carbon atoms of -COOH groups (Figure 4A).

A signal in the region of 9.8–10.3 ppm in the ^{31}P NMR spectrum of CPPP (Figure 2C) indicates the preservation of the phosphazene ring during the Doebner condensation, and it should be noted that the number of peaks in the multiplet decreases compared to the FPPP signal. It was assumed that one or more derivatives formed during the reaction would be removed from the overall mixture. However, based on the MALDI-TOF mass spectrum of CPPP (Figure 4B), the resulting mixture, like CPP and FPPP, consists of aryloxyphosphazenes containing 2 to 4 phenoxy radicals per phosphazene molecule. Therefore, we can conclude that the mesomeric effect of the ethenyl group has less influence on the phosphorus atoms of the phosphazene ring than the aldehyde ones, so the multiplet signals simply overlap.
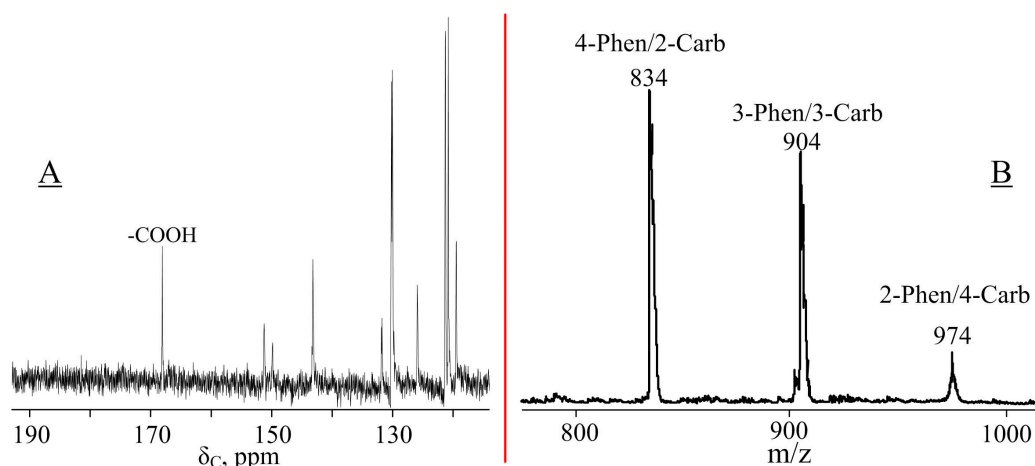
Figure 4. ^{13}C NMR (**A**) and MALDI-TOF (**B**) spectra of CPPP.

As a result of molecular modeling, it was found that the diameters of the sphere described around the molecule for all derivatives included in CPPP were about 2 nm (Table 1). Accordingly, the resulting carboxycyclotriphosphazenes can be considered nanosized modifiers of polymer materials.

Table 1. Values of the diameters of the sphere described around the molecules of di-, tri-, and tetra-derivatives contained in CPPP. The structures of CPPP and phosphazene intermediates are presented in the Supplementary Material (Table S1).

Contained in CPPP Derivative	Diameter of Sphere, nm
Nongem-cis-bis[4-(β-carboxyethenyl)phenoxy]-tetraphenoxycyclotriphosphazene	1.34
Nongem-trans-bis[4-(β-carboxyethenyl)phenoxy]-tetraphenoxycyclotriphosphazene	1.98
Nongem-cis-tris[4-(β-carboxyethenyl)phenoxy]-triphenoxycyclotriphosphazene	1.68
Nongem-trans-tris[4-(β-carboxyethenyl)phenoxy]-triphenoxycyclotriphosphazene	1.90
Gem-tris[4-(β-carboxyethenyl)phenoxy]-triphenoxycyclotriphosphazene	1.91
Nongem-cis-tetrakis[4-(β-carboxyethenyl)phenoxy]-diphenoxycyclotriphosphazene	1.93
Nongem-trans-tetrakis[4-(β-carboxyethenyl)phenoxy]-diphenoxycyclotriphosphazene	1.89

Using DSC, it was established that CPPP is amorphous, and its glass transition temperature is about 50 °C, which is obvious due to the presence of a second-order phase transition in the thermogram (Figure 5).

With further heating, no thermal effects are observed up to a temperature of 250 °C, above which a smooth exothermic effect with a maximum at 280 °C and simultaneous loss of mass by the sample begin, as follows from the TGA curve. This exotherm is caused by the process of decarboxylation and polymerization of the resulting styrene fragments [36]. Based on its amorphous structure, low softening point, and high thermal stability, CPPP can be considered as a potential hardener for epoxy resins with a wide operating temperature range.

To determine the curability of DER-331 resins, their mutual solubility should be assessed. This was achieved using the optical interferometry method (Figure 6). For the experiment, industrial epoxy resin brand DER-331 was used, since it is the most widely used, accessible, and cheap.

As follows from the interference patterns, complete interdiffusion of the components is achieved in 24 min at 80 °C; when the temperature rises to 130 °C, the process occurs in 10 min. It is worth noting that at 130 °C, simultaneously with the dissolution of the components, the curing process begins, which is completed in exactly 4 h; the gel fraction during this time reaches 99.5%.
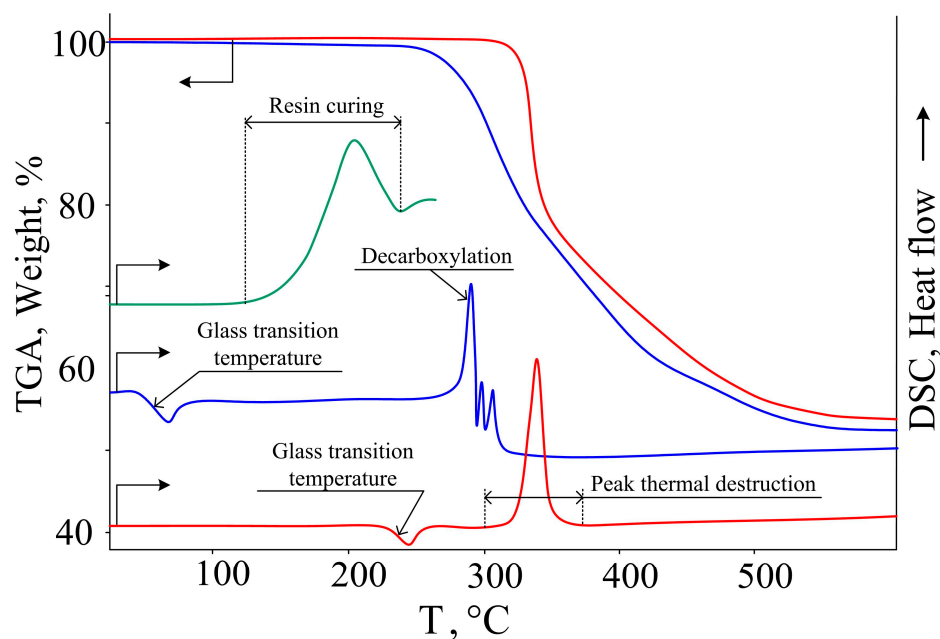
Figure 5. TGA and DSC curves of CPPP (blue), cured composition (red), and DSC curve of uncured composition (green).
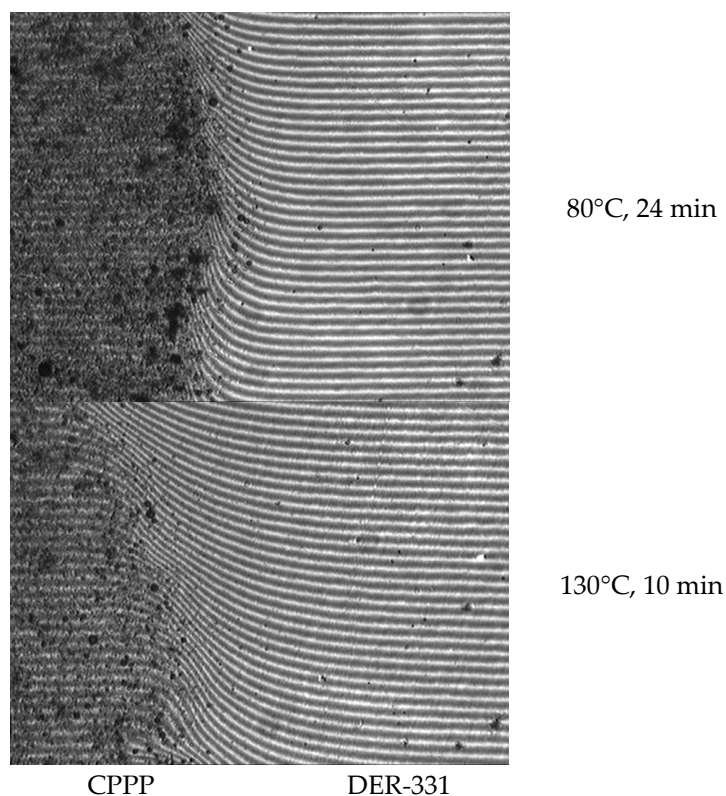

Figure 6. The interference pattern of the interdiffusion zones of CPPP and DER-331.

To evaluate the completeness of curing under the selected conditions of the epoxy resin, the conversion of epoxy groups was determined using IR spectroscopy. Comparing the spectra of the original resin (Figure 7) and the cured composition, one can observe the disappearance of bands in the cured sample characteristic of symmetrical (920 cm^{-1}) and stretching (820 cm^{-1}) vibrations of oxirane rings (Figure 7). In addition, in the spectrum of the final product in the region of 1150–1240 cm^{-1}, a "trident" is observed: a group of

signals characteristic of vibrations of the phosphazene ring. A similar "trident" is observed in the original CPPP, which indicates that the phosphazene cycle is maintained during the curing of the resin.
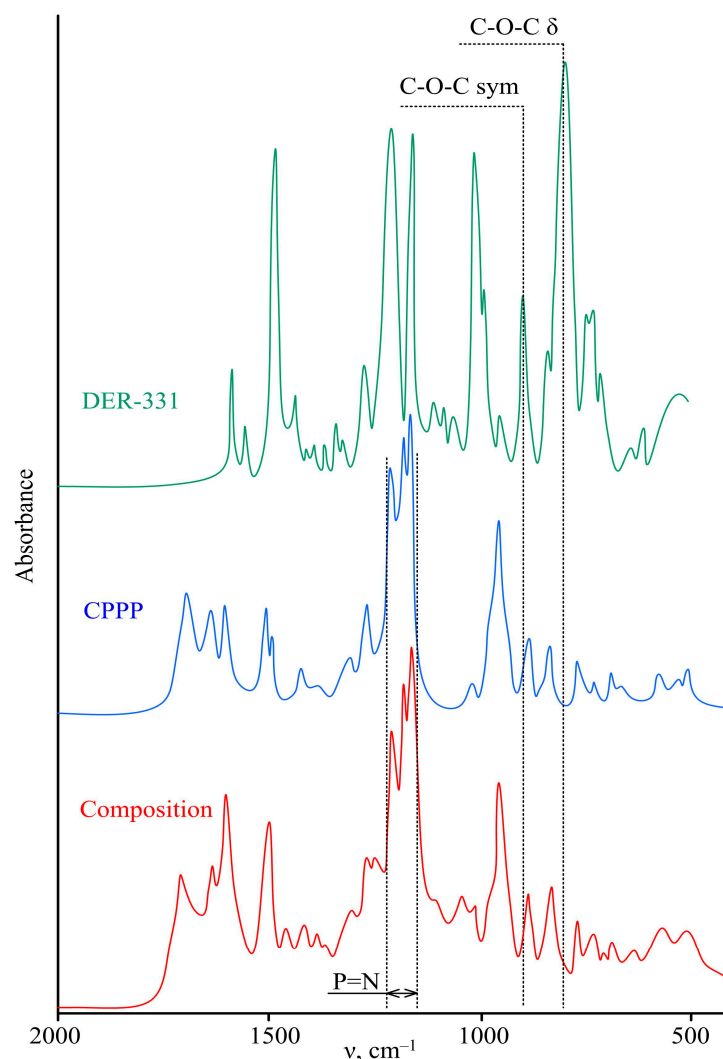

Figure 7. IR spectra of the initial components and the cured composition.

Using the DSC method (Figure 5), the glass transition temperature of the cured composition was determined, which was 230 °C, which is a fairly high-performance indicator of the material, since in most cases the areas of application of epoxy resins are determined precisely by the glass transition temperature. Such a high value is most likely due to the highly networked structure of the polymer formed during the curing process as well as the rigidity of its structure due to conjugation in the phosphazene ring and β-carboxyethenyl groups (Figure 8).

For comparison, the glass transition temperature of isophoronediamine-cured DER-331 resin is 110 °C.

Since almost one and a half times the mass excess of CPPP is used to cure the DER-331 resin, the composition based on them is solid at room temperature, and its melt has a very high viscosity, which limits the methods of processing and application of the material. The composition has the greatest prospects for use as an adhesive base for metals, since carboxyl groups can increase adhesive characteristics.
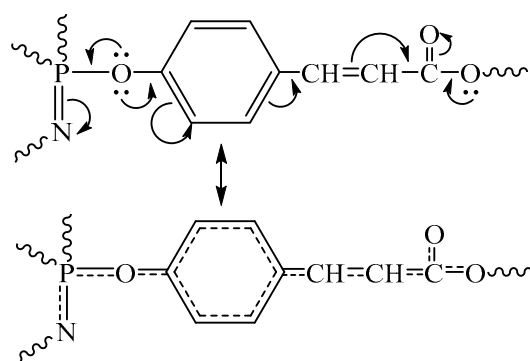
Figure 8. Conjugation of phosphazene ring and β-carboxyethenyl groups.

To evaluate adhesion, grade St3 steel and aluminum plates were glued together, and the strength of the adhesive seam was tested using the shear method. In this case, a cohesive rupture was visually observed, and the strength was 11 ± 0.2 MPa for both steel and aluminum. This also confirms the destruction of the composition itself and not its separation from the metals. Images of samples before and after testing are presented in the Supplementary Material (Figure S1).

When testing the composition for water absorption for 8 days, it was found that the amount of distilled water sorbed by the sample was about 2 wt.%, which is relatively small, despite the presence of polar hydroxyl groups in the substance. After the sample was dried, the weight loss was within the experimental error. When the sample was kept in salt water for 8 days, the weight loss also did not exceed the experimental error.

According to TGA data (Figure 5), the heat resistance of the cured composition was about 300 °C. When assessing fire resistance, it was established that the cured composition did not support combustion either with horizontal (burning time 20 s) or vertical (burning time 1 s) methods of fixing samples and did not form burning drops and, therefore, belonged to materials of the highest category of resistance to combustion V–0.

During the combustion process itself, abundant soot is released, and a dense coke cap is formed on the sample (Figure 9). In this case, the coke is porous and lacy, which is typical for most polymer thermosets modified with phosphazenes. Thanks to the porous, durable coke cap on the surface of the polymer, heat transfer from the flame into the depth of the sample is reduced. It is also clear from the microphotographs that the coke pores have a size of less than 10 nm and are closed, which prevents oxygen from accessing the material and, therefore, prevents combustion.
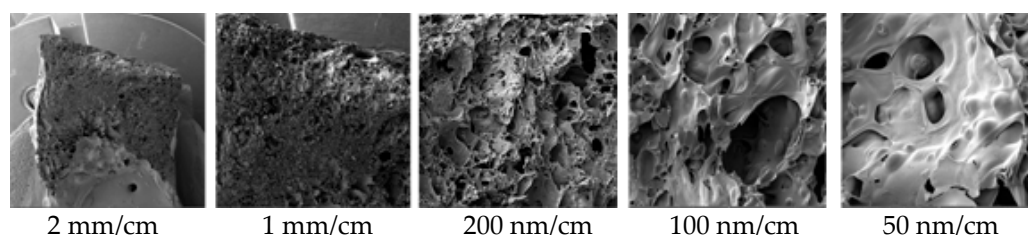

| 2 mm/cm | 1 mm/cm | 200 nm/cm | 100 nm/cm | 50 nm/cm |

Figure 9. A micrograph of a coke cap formed during a combustion test of a composition based on DER-331 and CPPP. Images of the samples before, after, and during testing are presented in the Supplementary Material (Figure S2).

Thus, we can conclude that the fire-retardant properties of the composition are achieved due to the cooperative effect of the phosphazene component: nitrogen ensures the foaming of the material, and phosphorus promotes the formation of a strong coke cap.

4. Conclusions

The goal of the work was to develop an epoxy composition with high adhesion to steel and aluminum, which at the same time has high fire resistance, thermal stability, heat resistance, resistance to fresh and salt water, and low water absorption. To obtain such a composition, aryloxycyclophosphazenes CPPP, containing phenoxy and β-carboxyethenylphenoxy radicals at the phosphorus atoms of the phosphazene ring, were used as a curing agent.

CPPPs are an amorphous rather than crystalline substance, highly soluble in DER-331 epoxy-diane resin, which allows the composition to be obtained at a lower temperature than when the resin begins to cure.

Due to the presence of carboxyl groups in the phosphazene hardener, the resulting polymer has high shear strength of the adhesive bond to steel and aluminum (11 ± 0.2 MPa). In turn, the cooperative effect of the phosphorus and nitrogen atoms of the phosphazene ring provides the material with a V–0 criterion in the UL-94 vertical combustion test due to a phosphorus content of 6 wt. %, which indicates a high fire resistance of the polymer.

The developed epoxy composition can be used as a highly adhesive non-flammable hot-curing adhesive, for example, for gluing metal structures in the aircraft industry, binders for RTM and VARTM processes for pre-treatment of metal or metal oxide fillers, or fire-retardant coatings for electrical equipment, ships, and building structures.

In the future, a study is planned of a number of mechanical and rheological properties and new approaches to the process of curing compositions to assess the prospects for their use in innovative fields of technology [40,41].

Supplementary Materials: The following supporting information can be downloaded at https://www.mdpi.com/article/10.3390/sci6020030/s1. Figure S1: Testing samples for adhesion strength; Figure S2: Testing samples for combustion resistance (A—bringing a flame to the sample; B—combustion process; C—self-extinguishing; D—original sample; E—sample after combustion); Table S1: Values of the diameters of the sphere described around molecules of di-, tri-, and tetra-derivatives contained in CPP, FPPP, and CPPP and their mole fractions.

Author Contributions: Conceptualization, E.C.; methodology, E.C.; validation, A.P. and P.Y.; investigation, D.P., A.K., A.S., P.Y., E.C. and A.P.; resources, P.Y.; data curation, A.K.; writing—original draft preparation, E.C.; writing—review and editing, E.C. and P.Y.; visualization, E.C.; supervision, E.C.; project administration, E.C.; funding acquisition, E.C. All authors have read and agreed to the published version of the manuscript.

Informed Consent Statement: Informed consent was obtained from all subjects involved in the study.

Data Availability Statement: The data presented in this study are available on request from the corresponding author.

Conflicts of Interest: The authors declare no conflicts of interest.

References

1. Lopes, P.E.; Moura, D.; Hilliou, L.; Krause, B.; Pötschke, P.; Figueiredo, H.; Alves, R.; Lepleux, E.; Pacheco, L.; Paiva, M.C. Mixed carbon nanomaterial/epoxy resin for electrically conductive adhesives. *J. Compos. Sci.* **2020**, *4*, 105. [CrossRef]
2. Li, S.; Cui, H.; Wang, H.; Wang, W.; Sui, Y.; Dong, L.; Wang, J. Preparation and performance investigation of epoxy resin-based permeable concrete containing ceramsite. *Polymers* **2023**, *15*, 4704. [CrossRef]
3. Wu, Y.; Fan, X.; Wang, Z.; Zhang, Z.; Liu, Z. A mini-review of ultra-low dielectric constant intrinsic epoxy resins: Mechanism, preparation and application. *Polym. Adv. Tecnol.* **2024**, *35*, 6241. [CrossRef]
4. Zhang, K.; Huang, J.; Wang, Y.; Li, W.; Nie, X. Eco-friendly epoxy-terminated polyurethane-modified epoxy resin with efficient enhancement in toughness. *Polymers* **2023**, *15*, 2803. [CrossRef]

5. Siahtiri, S.; Sahraei, A.A.; Mokarizadeh, A.H.; Baghani, M.; Bodaghi, M.; Baniassadi, M. Influence of curing agents molecular structures on interfacial characteristics of graphene/epoxy nanocomposites: A molecular dynamics framework. *Macromol. Mater. Eng.* **2023**, *308*, 2300030. [CrossRef]

6. Zhang, L.; Liu, J.; Dai, J.; Zhang, X.; Liu, X.; Liu, X.; Yi, X. Preparation and application of a multifunctional interfacial modifier for ramie fiber/epoxy resin composites. *Polymers* **2023**, *15*, 3800. [CrossRef] [PubMed]

7. Akin, E.; Çakir, M.; Demirer, H. Multi-featured epoxy composites filled with surface-modified PTFE powders treated by Na-naphthalenide system. *J. Appl. Polym. Sci.* **2024**, *141*, 54947. [CrossRef]

8. Kim, Y.; Lee, S.; Yoon, H. Fire-safe polymer composites: Flame-retardant effect of nanofillers. *Polymers* **2021**, *13*, 540. [CrossRef]

9. Yang, X.; Zhang, Y.; Chen, J.; Zou, L.; Xing, X.; Zhang, K.; Liu, J.; Liu, X. Flame-retardant thermoplastic polyether ester/aluminum butylmethylphosphinate/phenolphthalein composites with enhanced mechanical properties and antidripping. *Polymers* **2024**, *16*, 552. [CrossRef] [PubMed]

10. Liu, Y.; Tang, Z.; Zhu, J. Synergistic flame retardant effect of aluminum hydroxide and ammonium polyphosphate on epoxy resin. *J. Appl. Polym. Sci.* **2022**, *139*, 53168. [CrossRef]

11. Shi, C.; Wan, M.; Qian, X.; Jing, J.; Zhou, K. Zinc Hydroxystannate/carbon nanotube hybrids as flame retardant and smoke suppressant for epoxy resins. *Molecules* **2023**, *28*, 6820. [CrossRef] [PubMed]

12. Lv, Y.F.; Thomas, W.; Chalk, R.; Singamneni, S. Flame retardant polymeric materials for additive manufacturing. *Mater. Today Proc.* **2020**, *33*, 5720–5724. [CrossRef]

13. Zhang, X.; Wang, Z.; Xie, J. Synthesis and curing properties of fluorinated curing agent for epoxy resin based on natural soybean isoflavones. *React. Funct. Polym.* **2023**, *184*, 105511. [CrossRef]

14. Benmammar, R.K.; Mundlapati, V.R.; Bouberka, Z.; Barrera, A.; Staelens, J.-N.; Tahon, J.-F.; Ziskind, M.; Carpentier, Y.; Focsa, C.; Supiot, P.; et al. Electron beam processing as a promising tool to decontaminate polymers containing brominated flame retardants. *Molecules* **2023**, *28*, 7753. [CrossRef] [PubMed]

15. Cai, G.; Wan, Y.; Liu, J.; Yang, N.; Guo, J.; Li, J.; Zou, Y.; Zhan, J.; Zhan, H.; Wang, M. Preparation and performance analysis of methyl-silicone resin-modified epoxy resin-based intumescent flame retardant thermal insulation coating. *J. Micromechanics Mol. Phys.* **2023**, *8*, 61–82. [CrossRef]

16. Tavakoli, M.; Mazela, B.; Grześkowiak, W.; Proch, J.; Mleczek, M.; Perdoch, W. The strength and fire properties of paper sheets made of phosphorylated cellulose fibers. *Molecules* **2024**, *29*, 133. [CrossRef]

17. Dou, Y.; Zhong, Z.; Huang, J.; Ju, A.; Yao, W.; Zhang, C.; Guan, D. A new phosphorous/nitrogen-containing flame-retardant film with high adhesion for jute fiber composites. *Polymers* **2023**, *15*, 1920. [CrossRef]

18. Davidson, D.J.; McKay, A.P.; Cordes, D.B.; Woollins, J.D.; Westwood, N.J. The covalent linking of organophosphorus heterocycles to date palm wood-derived lignin: Hunting for new materials with flame-retardant potential. *Molecules* **2023**, *28*, 7885. [CrossRef] [PubMed]

19. Chai, H.; Li, W.; Wan, S.; Liu, Z.; Zhang, Y.; Zhang, Y.; Zhang, J.; Kong, Q. Amino phenyl copper phosphate-bridged reactive phosphaphenanthrene to intensify fire safety of epoxy resins. *Molecules* **2023**, *28*, 623. [CrossRef]

20. Ma, X.; Kang, N.; Zhang, Y.; Min, Y.; Yang, J.; Ban, D.; Zhao, W. Enhancing flame retardancy and smoke suppression in epoxy resin composites with sulfur–phosphorous reactive flame retardant. *Molecules* **2024**, *29*, 227. [CrossRef]

21. Li, P.; Wang, J.; Wang, C.; Xu, C.; Ni, A. The flame retardant and mechanical properties of the epoxy modified by an efficient DOPO-based flame retardant. *Polymers* **2024**, *16*, 631. [CrossRef]

22. Wang, W.; Wang, F.; Li, H.; Liu, Y. Synthesis of phosphorus-nitrogen hybrid flame retardant and investigation of its efficient flame-retardant behavior in PA6/PA66. *J. Appl. Polym. Sci.* **2023**, *140*, 53536. [CrossRef]

23. Li, K.; Gao, Y.; Li, X.; Zhang, Y.; Zhu, B.; Zhang, Q. Fragmentation pathway of organophosphorus flame retardants by liquid chromatography–orbitrap-based high-resolution mass spectrometry. *Molecules* **2024**, *29*, 680. [CrossRef] [PubMed]

24. Akbaş, H.; Şenocak, A.; Kılıç, Z.; Tayhan, S.E.; Bilgin, S.; Yıldırım, A.; Hökelek, T. Syntheses of tetrachloro and tetraamino (2-furanylmethyl) spiro (N/N) cyclotriphosphazenes: Chemical, structural elucidation, antiproliferative and antimigratory activity studies. *J. Mol. Struct.* **2023**, *1282*, 135209. [CrossRef]

25. Koran, K.; Çalışkan, E.; Öztürk, D.A.; Çapan, İ.; Tekin, S.; Sandal, S.; Görgülü, A.O. The first peptide derivatives of dioxybiphenyl-bridged spiro cyclotriphosphazenes: In vitro cytotoxicity activities and DNA damage studies. *Bioorg. Chem.* **2023**, *132*, 106338. [CrossRef]

26. Serbezeanu, D.; Vlad-Bubulac, T.; Macsim, A.M.; Bălan, V. Design and synthesis of amphiphilic graft polyphosphazene micelles for docetaxel delivery. *Pharmaceutics* **2023**, *15*, 1564. [CrossRef]

27. Zhao, X.; Liu, Z.; Zhang, S.; Hassan, M.; Ma, C.; Liu, Z.; Gong, W. Synthesis of pillar[5]arene-and phosphazene-linked porous organic polymers for highly efficient adsorption of uranium. *Molecules* **2023**, *28*, 1029. [CrossRef] [PubMed]

28. Piskun, Y.A.; Ksendzov, E.A.; Resko, A.V.; Soldatov, M.A.; Timashev, P.; Liu, H.; Vasilenko, I.V.; Kostjuk, S.V. Phosphazene functionalized silsesquioxane-based porous polymer as thermally stable and reusable catalyst for bulk ring-opening polymerization of ε-caprolactone. *Polymers* **2023**, *15*, 1291. [CrossRef]

29. Dagdag, O.; Kim, H. Progress in the field of cyclophosphazenes: Preparation, properties, and applications. *Polymers* **2023**, *16*, 122. [CrossRef]

30. Bao, D.M.; Wang, J.H.; Hou, Z.M.; Xu, Z.Y.; Ye, X.L.; Qi, Y.Z.; Wen, Z. Synthesis of a novel flame retardant with phosphaphenanthrene and phosphazene double functional groups and flame retardancy of poly (lactic acid) composites. *Front. Mater.* **2022**, *9*, 951515. [CrossRef]

31. Mayer-Gall, T.; Plohl, D.; Derksen, L.; Lauer, D.; Neldner, P.; Ali, W.; Fuchs, S.; Gutmann, J.S.; Opwis, K. A green water-soluble cyclophosphazene as a flame retardant finish for textiles. *Molecules* **2019**, *24*, 3100. [CrossRef] [PubMed]

32. Tian, L.; Zheng, Q.; Zeng, H.; Wang, X.; Cui, J.; Yang, B.; Guo, J.; Mu, B.; Bao, X.; Wan, X.; et al. Synthesis of multi-element hybrid polyphosphonitrile microspheres and their flame retardant application in epoxy resins. *J. Appl. Polym. Sci.* **2023**, *140*, 54668. [CrossRef]

33. Xu, B.; Wu, M.; Liu, Y.; Wei, S. Study on flame retardancy behavior of epoxy resin with phosphaphenanthrene triazine compound and organic zinc complexes based on phosphonitrile. *Molecules* **2023**, *28*, 3069. [CrossRef]

34. Tang, S.; Qian, L.; Liu, X.; Dong, Y. Gas-phase flame-retardant effects of a bi-group compound based on phosphaphenanthrene and triazine-trione groups in epoxy resin. *Polym. Degrad. Stab.* **2016**, *133*, 350–357. [CrossRef]

35. Waldin, N.A.; Jamain, Z. The effect of alkyl terminal chain length of Schiff-based cyclotriphosphazene derivatives towards epoxy resins on flame retardancy and mechanical properties. *Polymers* **2023**, *15*, 1431. [CrossRef] [PubMed]

36. Chistyakov, E.M.; Panfilova, D.V.; Kireev, V.V.; Volkov, V.V.; Bobrov, M.F. Synthesis and properties of hexakis-(β-carboxyethenylphenoxy)cyclotriphosphazene. *J. Mol. Struct.* **2017**, *1148*, 1–6. [CrossRef]

37. *ISO 4587:1979*; Adhesives—Determination of Tensile Lap-Shear Strength of High Strength Adhesive Bonds. ISO: Geneva, Switzerland, 1979.

38. *ISO 62:2008*; Plastics—Determination of Water Absorption. ISO: Geneva, Switzerland, 2008.

39. *ISO 175:2010*; Plastics—Methods of Test for the Determination of the Effects of Immersion in Liquid Chemicals. ISO: Geneva, Switzerland, 2010.

40. Wang, T.P.; Shen, L.; Forrester, M.; Lee, T.H.; Torres, S.; Pearson, C.; Cochran, E. Shelf-stable Bingham plastic polyurethane thermosets for additive manufacturing. *ACS Mater. Lett.* **2024**, *6*, 1077–1085. [CrossRef]

41. Shen, L.; Wang, T.P.; Lee, T.H.; Forrester, M.; Becker, A.; Torres, S.; Cochran, E.W. 3D printable all-polymer epoxy composites. *ACS Appl. Polym. Mater.* **2021**, *3*, 5559–5567. [CrossRef]